Wideband Stacked Patch Antenna Array on LTCC for W-Band

Antti Lamminen and Jussi Säily
VTT Technical Research Centre of Finland
P.O. Box 1000, FI-02044 VTT, Finland
antti.lamminen@vtt.fi, jussi.saily@vtt.fi

***Abstract*—A design of a stacked microstrip patch antenna and a 16-element array on Ferro A6-M LTCC operating at W-band is presented. A parasitic patch is added on LTCC substrate to increase bandwidth. The stacked configuration is designed by using an equivalent circuit together with EM simulators. The manufactured antenna array is integrated with a WR-10-to-microstrip-line transition to facilitate RF testing. The S-parameters are measured on a probe station and radiation pattern testing is done using a WR-10 excitation in anechoic chamber. The array of size 9.3 mm $\times$ 9.3 mm $\times$ 0.4 mm has the measured maximum gain of 14.2 dBi at 84 GHz and gain higher than 11.2 dBi between 78.5 GHz and 98.5 GHz which results as -3-dB radiation bandwidth of 23%. The antenna efficiency of the array is 48% at the highest.**

I. Introduction

The increasing need for higher data rates in consumer applications has raised a lot of interest in developing low-cost radio solutions for 60 GHz and E-band (71–86 GHz) frequencies. The low temperature co-fired ceramic (LTCC) technology has been widely used to fabricate millimetre-wave antennas operating at frequencies up to 94 GHz [1]. Patch antennas are commonly used in array configuration to increase antenna gain. However, antennas on LTCC substrates often suffer from narrow bandwidth due to the high-permittivity substrate. One method to increase the bandwidth is to process air cavities inside LTCC to decrease the effective dielectric constant [2]. The drawback is a more complicated structure which increases manufacturing costs.

It is known that parasitic patches can be used for dual-frequency operation [3] and to increase the bandwidth. In [4] a parasitic patch array design has been developed for 60 GHz on LTCC to increase the antenna gain. A gain of about 8 dBi and a bandwidth of 3.3% is reported for a 4-element array excited with a single antenna element. In this work, parasitic patches are used to increase the bandwidth of a patch antenna and a 16-element array operating at W-band (75–110 GHz).

A wideband transition from a WR-10 waveguide to a microstrip line (WG-MS) with similar topology as the parasitic patch array is used to facilitate radiation pattern testing. The developed antennas have wideband impedance and radiation characteristics with medium antenna gain. For verification of the design, simulated and measured S-parameter and radiation pattern results of fabricated antenna prototypes are presented.

II. Stacked Patch Antenna Design

In this section, the design procedure of a stacked patch antenna is described. There are many different parameters to be optimised due to two resonating patches. An equivalent circuit is useful when investigating the behaviour of the antenna and can be used to minimise the number of iterations with an EM simulator.

A. Single-Resonant Antenna

First, a single-resonant antenna is designed on an LTCC substrate. The tape thickness of used Ferro A6-M LTCC material is around 0.1 mm so only discrete values $N \times 0.1$ mm of substrate thicknesses are possible where N is the number of tape layers. From Fig. 2 in [5] one can estimate that with $\epsilon_r = 6$ the substrate thickness of $h \leq 0.06\lambda_0$ should be chosen to obtain an efficieny above 60%. At the center frequency of the W-band, 93 GHz, this results as $h \leq 0.2$ mm. The value $h = 0.2$ mm is chosen.

An aperture-coupled patch antenna is optimised for a center frequency of 93 GHz using Zeland IE3D. The developed antenna consists of three Ferro A6-M LTCC tape layers having $\epsilon_\mathrm{r} = 5.7$ and $\tan\delta = 0.0015$. Used gold paste has $\sigma_{\mathrm{Aup}} = 7.0 \cdot 10^6$ S/m. The dimensions of the antenna are: $l_{ap} = 0.32$, $l_p = w_p = 0.5$, $l_s = 0.275$, and $w_{ms} = 0.144$ (mm). The $|S_{11}| \leq -10$ dB impedance band is between 88.5 GHz and 95.5 GHz resulting as an impedance bandwidth of $B_{sr} = 7.6\%$. The maximum gain is about 2.7 dBi.

B. Equivalent Circuit

An equivalent circuit for a dual-resonant patch antenna shown in Fig. 1 has been proposed in [6]. The parallel (B) and series (D) RLC-circuits model the driven patch and the parasitic patch. The first transformer (A) represents the coupling between the feed line and the driven patch. The second transformer (C) represents the coupling between the two patches. In Fig. 1 the feed inductance is excluded. The n_1 is increased when the size of the aperture is increased or the distance between the feed and the driven patch is decreased. Similarly, n_2 can be controlled with the separation between patches. The component values of the resonators can be calculated using (1)–(5) in [6].

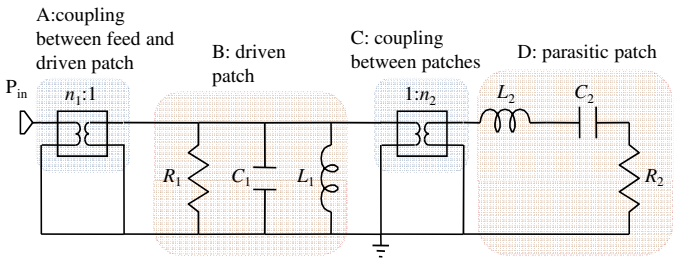

Fig. 1. Equivalent circuit for dual-resonant patch antenna.

C. Dual-Resonant Antenna

The design of a stacked patch antenna can be started from the optimised single-resonant antenna. The unloaded Q-value Q_0 can be calculated from (5) in [6]. When selecting $S \leq 2$ for *VSWR* and $B_{sr} = 0.076$, this results as $Q_0 = 9.9$. Let us choose the same resonance frequencies for both patches, i.e., $f_{r1} = f_{r2} = 93$ GHz. Let us assume the same quality factors for both patches, i.e., $Q_{01} = Q_{02} = Q_0 = 9.9$ and $R_1 = R_2$ = 50 Ω. By using (2) and (3) in [6] this leads to $C_1 = 0.339$ pF, $L_1 = 8.643$ pH, $C_2 = 0.00346$ pF and $L_2 = 847.1$ pH.

The equivalent circuit was implemented in the AWR Microwave Office circuit simulator. The turns ratios n_1 and n_2 of the transformers were optimised for the maximum bandwidth. This results as $n_1 = 1.8$ and $n_2 = 2.3$. By excluding the parasitic patch, the input impedance for the driven patch can be estimated. In this particular case, the input resistance is 162 Ω at 93 GHz. The patch is overcoupled which is seen as a large input impedance loop on a Smith chart (Fig. 2b, red dashed line). This indicates that the driven patch should be closer to the feed line than the optimised single-resonant patch (optimisation was done to 50 Ω). It is seen from n_1 and n_2 values that coupling from the feed to the driven patch is of the same order than coupling from the driven patch to the parasitic patch. It is observed from Fig. 2a that the $|S_{11}|$ of the stacked patch is below -10 dB between 82 GHz and 105 GHz. For the driven patch alone, the $|S_{11}|$ is about -5.5 dB at the minimum.

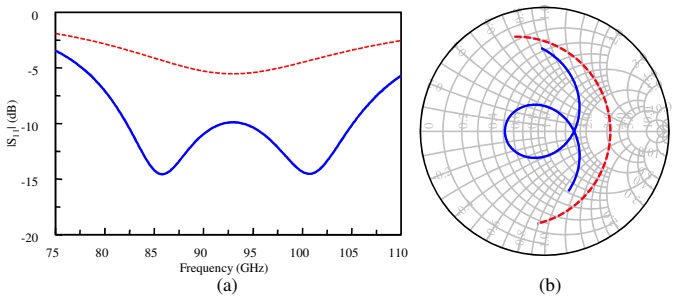

Fig. 2. Results of a stacked patch antenna using equivalent circuit. (a) Reflection coefficient, (b) input impedance. Red dashed line is for driven patch only and blue solid line is for the whole dual-resonant antenna.

The stacked patch is designed using Zeland IE3D. The size of the single-resonant patch is scaled down in geometry to maintain $f_{r1} = 93$ GHz inside substrate and the driven patch is placed closer to the feed line, i.e. $h_{p1} = 0.1$ mm. After optimising the driven patch alone for a 0.3 mm thick substrate, it is observed that the required $R_{in} \approx 160$ Ω is achieved with $l_p = w_p = 0.4$ and $l_{ap} = 0.38$ (mm). Finally, the parasitic patch of size $l_p = w_p = 0.5$ mm is placed on top of the substrate ($h_{p2} = 0.3$ mm). Two resonances are observed in the $|S_{11}|$ curve and the input impedance loop is centered on a Smith chart. If slightly misaligned, the loop could be shifted towards center by properly adjusting the resonance frequencies of the patches, i.e., the patch sizes.

D. Prototype Designs

The final optimisation of the stacked patch antenna was done using Ansoft HFSS. Optimised antenna dimensions are (in mm): $l_{\text{p1}} = 0.415$, $l_{\text{p2}} = 0.475$, $h = 0.097$, $t = 0.008$, $w_{\text{ms}} = 0.13$, $l_{\text{s}} = 0.245$, and $l_{\text{ap}} = 0.355$. The $|S_{11}| \leq -10$ dB between 77 GHz and 110 GHz. The maximum gain varies between 1.8 dBi and 4.3 dBi peaking at 80 GHz. The radiation efficiency is between 82% and 90%. Simulation results are shown in Fig 3. It is seen that the reflection coefficients are very similar to the ones calculated using the equivalent circuit. In spite of the fact that the parameter values used in the equivalent circuit are only approximations, the equivalent circuit is useful for getting a draft design of a dual-resonant patch antenna.

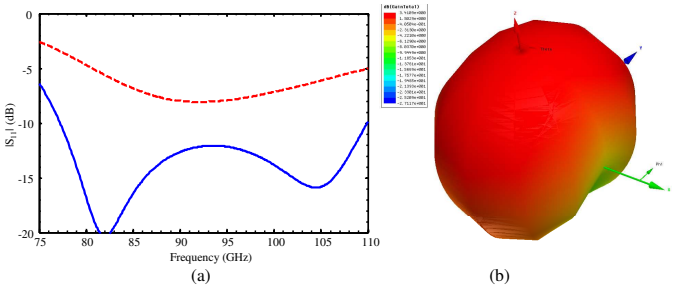

Fig. 3. Simulation results of a stacked patch antenna. (a) $|S_{11}|$ for the driven patch (red dashed line) and for the stacked patch antenna (blue solid line). (b) 3D gain pattern at 94 GHz. The maximum gain is 3.4 dBi.

A 16-element stacked patch antenna array of size $D = 9.3$ mm and an element separation of $d = 2$ mm was also designed (see Fig. 4). Microstrip line feed network with Wilkinson power dividers was optimised for the center frequency of 93 GHz. The required 100-Ω resistors are screen-printed on LTCC using a resistive paste. The simulated return loss of the Wilkinson was higher than 10 dB at all ports between 75 GHz and 107 GHz. Accordingly, the input-to-output losses remained below 1 dB and the isolation between output ports below -13 dB across the band.

For RF testing of the manufactured prototype, the array was integrated with the WG-MS transition described in [7]. The transition is quite similar to the stacked patch antenna but vias are placed around patches to prevent power leakage. In addition, the impedance is optimised for the WR-10 waveguide. The transition was placed 22 mm apart from the center of the array to prevent waveguide flange from disturbing antenna

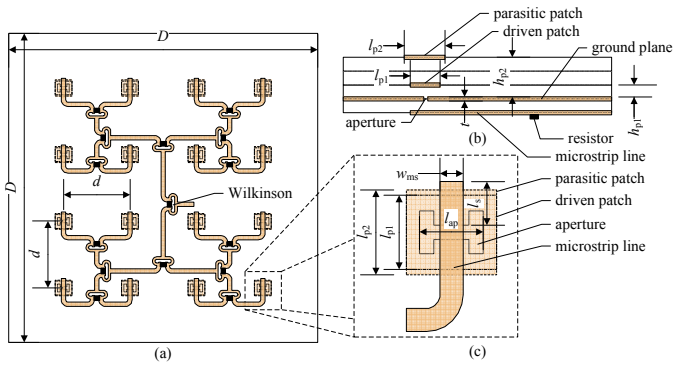

Fig. 4. Antenna geometry. a) top view of the array, b) LTCC layer structure, c) top view of an array element.

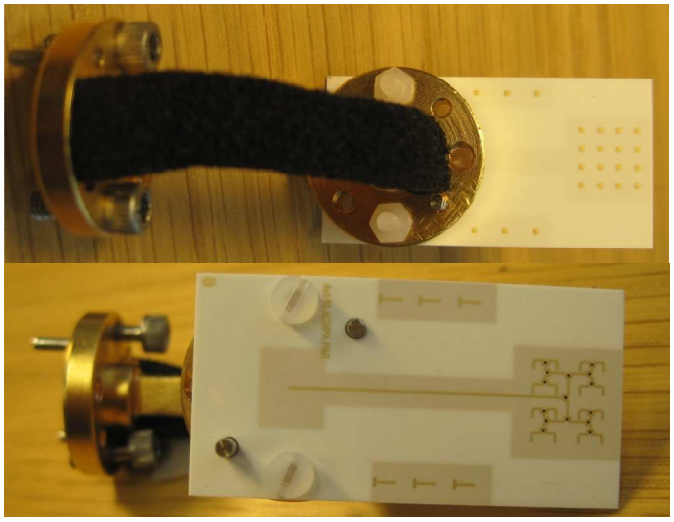

Fig. 5. Photographs of the antenna array connected to a WR-10 waveguide. (top) patches, (bottom) feed network.

radiation. Photographs of the LTCC antenna array connected to a WR-10 waveguide using nylon screws are shown in Fig. 5. RF absorber is glued on top of the WR-10 to prevent reflections.

III. Results

The S-parameters of the manufactured antennas were measured on a Cascade Microtech on-wafer probe station and HP 8510C vector network analyzer (VNA). The *TRL* calibration method was used. Simulated and measured reflection coefficients of a stacked patch antenna and a 16-element array are shown in Fig. 6. Dual-resonant behaviour is seen also in the measurement results of the element. The $|S_{11}|$ of the element is below -10 dB above 78 GHz. The reflection coefficient of the array is below -6 dB between 78 GHz and 108 GHz.

The radiation patterns were measured in an anechoic chamber at VTT. The measurement procedure is similar to the one previously used at V-band [2]. The HP 83557A mm-wave source module was replaced with an HP 83558A and the Agilent 11970V waveguide harmonic mixer with an Agilent 11970W. The radiation patterns of the array are displayed at

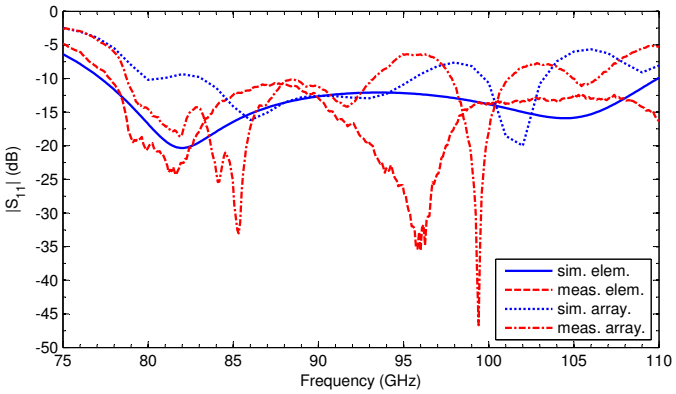

Fig. 6. Reflection coefficients of a single element and the array.

different frequencies in Figs. 7–12. The simulated and the measured results compare very well with each other. The suppressed side lobe in the H-plane results at negative angle values is due to the WR-10 waveguide blocking radiation. The maximum gain of 14.2 dBi is observed at 84 GHz. The cross-polarisation level is about -25 dB. The back-radiation level is -12 dB at the highest. The -3-dB beamwidth decreases with increasing frequency and varies between 18° and 26°.

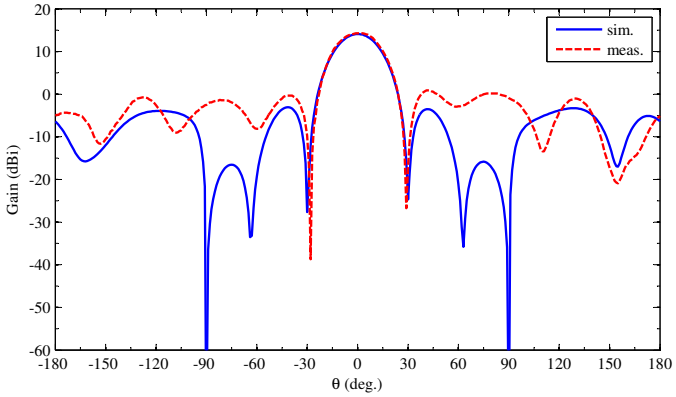

Fig. 7. Co-pol. E-plane radiation patterns at 84 GHz.

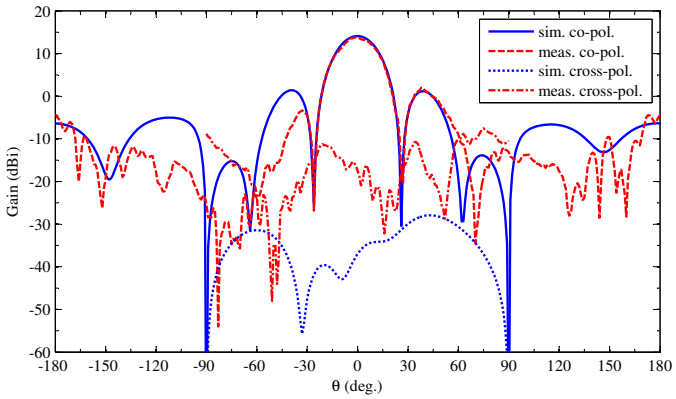

Fig. 8. Co-pol. and cross-pol. H-plane radiation patterns at 84 GHz.

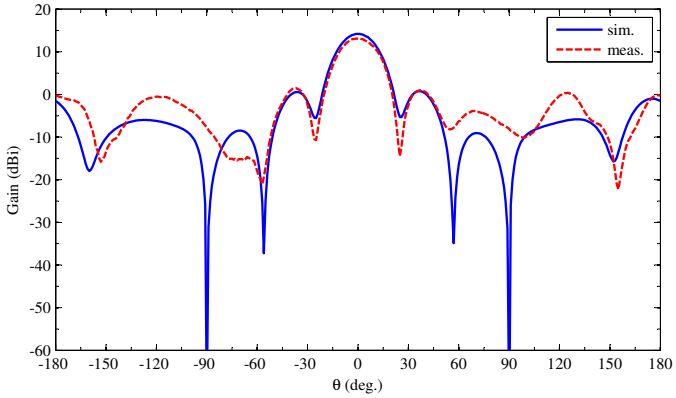

Fig. 9. Co-pol. E-plane radiation patterns at 90 GHz.

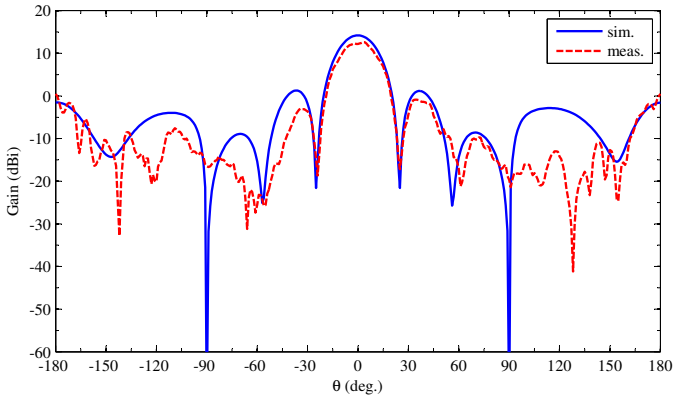

Fig. 10. Co-pol. H-plane radiation patterns at 90 GHz.

The maximum gain and directivity of the array as a function of frequency is shown in Fig. 13. The gain results include the feed-network losses (see Fig. 4). The -3-dB radiation bandwidth is between 78.5 GHz and 98.5 GHz. The small difference between simulated and measured results can be due to the effects of the surroundings, the losses of the transition and the errors in the gain reference. The antenna efficiency is 48% at the highest.

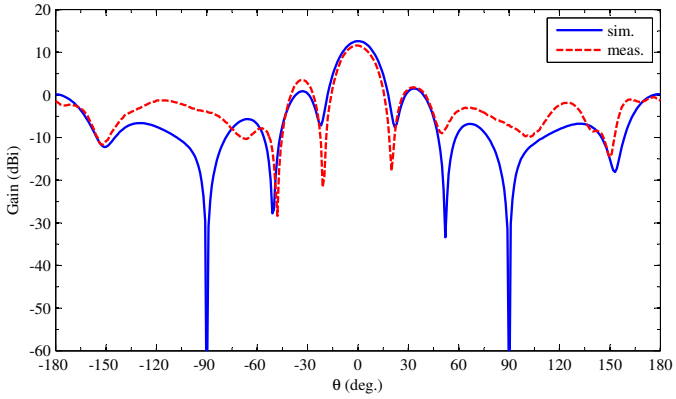

Fig. 11. Co-pol. E-plane radiation patterns at 96 GHz.

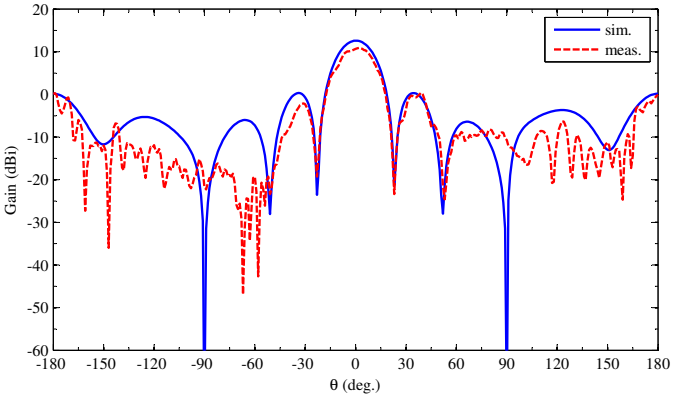

Fig. 12. Co-pol. H-plane radiation patterns at 96 GHz.

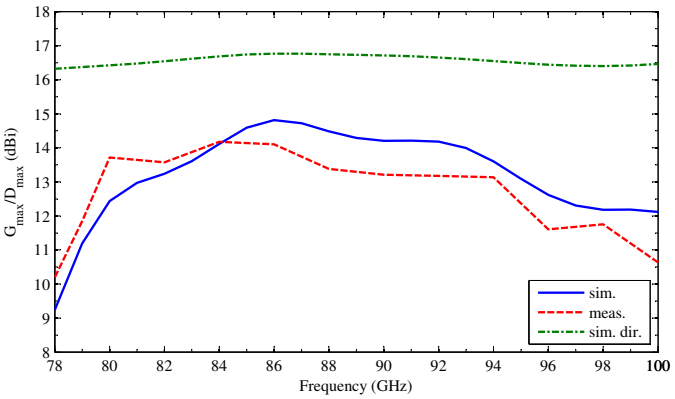

Fig. 13. Maximum gain of the antenna array. Simulated directivity is shown as dash-dot line.

IV. Conclusions

A wideband stacked microstrip patch antenna array on Ferro A6-M LTCC operating at W-band has been developed. A measured -3-dB radiation bandwidth of 23% and the maximum gain of 14.2 dBi are achieved for a 16-element array. The main benefit of the antenna is that wideband operation is achieved without any additional processing steps, such as drilling cavities inside substrate. The developed antenna can be easily scaled to lower frequencies, such as 60 GHz, by increasing the patch sizes, the coupling aperture, and the substrate thicknesses. The proposed antenna is a good candidate for high data rate short-range millimetre-wave applications such as radar, MMID, and indoor mm-wave WPAN base stations.

Acknowledgements

This work was supported by Tekes and the industrial members of the BRAWE project. The authors would like to thank VTT's LTCC-processing staff and Mr Hannu Hakojärvi and Mr Ismo Huhtinen for helping with the measurements.

References

[1] J. Aguirre, H.-Y. Pao, and H.-S. Lin, "An LTCC 94 GHz antenna array," in *IEEE Antennas and Propagation Society International Symposium*, San Diego, CA, July 2008, pp. 1–4.

[2] A. E. I. Lamminen, J. Säily, and A. R. Vimpari, "60-GHz patch antennas and arrays on LTCC with embedded-cavity substrates," *IEEE Trans. Antennas Propagat.*, vol. 56, no. 9, pp. 2865–2874, Sept. 2008.
[3] R. E. Munson, "Microstrip antennas," in *Antenna Engineering Handbook*, R. C. Johnson, Ed. New York: McGraw Hill, 1993, ch. 7.
[4] T. Seki, N. Honma, K. Nishikawa, and K. Tsunekawa, "A 60-GHz multilayer parasitic microstrip array antenna on LTCC substrate for system-on-package," *IEEE Microwave Wireless Compon. Lett.*, vol. 15, no. 5, pp. 339–341, May 2005.
[5] D. M. Pozar, "Microstrip antennas," *Proc. IEEE*, vol. 80, no. 1, pp. 79–91, Jan. 1992.
[6] J. Ollikainen and P. Vainikainen, "Design and bandwidth optimization of dual-resonant patch antennas," Helsinki University of Technology, Radio Laboratory publications, Espoo, Tech. Rep. S 252, 2002. [Online]. Available: http://lib.tkk.fi/Diss/2004/isbn9512273810/article1.pdf
[7] A. Lamminen and J. Säily, "77 GHz beam-switching high-gain end-fire antenna on LTCC," in *Proc. 20th International Conference on Applied Electromagnetics and Communications (ICECom 2010)*, Dubrovnik, Croatia, Sept. 2010.